Journal of Coordination Chemistry

ISSN: 0095-8972 (Print) 1029-0389 (Online) Journal homepage: http://www.tandfonline.com/loi/gcoo20

Saalfrank-type $\{Fe_2L_3\}$ host–guest complexes – prediction of ion selectivity by quantum chemical calculations VII

Svetlana Begel, Andreas Scheurer & Ralph Puchta

To cite this article: Svetlana Begel, Andreas Scheurer & Ralph Puchta (2015) Saalfrank-type $\{Fe_2L_3\}$ host–guest complexes – prediction of ion selectivity by quantum chemical calculations VII, Journal of Coordination Chemistry, 68:17-18, 3374-3387, DOI: 10.1080/00958972.2015.1076806

To link to this article: http://dx.doi.org/10.1080/00958972.2015.1076806

Accepted author version posted online: 30 Jul 2015.
Published online: 02 Sep 2015.

Journal of Coordination Chemistry, 2015
Vol. 68, Nos. 17–18, 3374–3387, http://dx.doi.org/10.1080/00958972.2015.1076806

Saalfrank-type $\{Fe_2L_3\}$ host–guest complexes – prediction of ion selectivity by quantum chemical calculations VII

SVETLANA BEGEL†, ANDREAS SCHEURER*† and RALPH PUCHTA*†‡

†Inorganic Chemistry, Department of Chemistry and Pharmacy, Universität Erlangen-Nürnberg, Erlangen, Germany
‡Department of Chemistry and Pharmacy, Computer Chemistry Center, Universität Erlangen-Nürnberg, Erlangen, Germany

(*Received 11 June 2015; accepted 22 July 2015*)

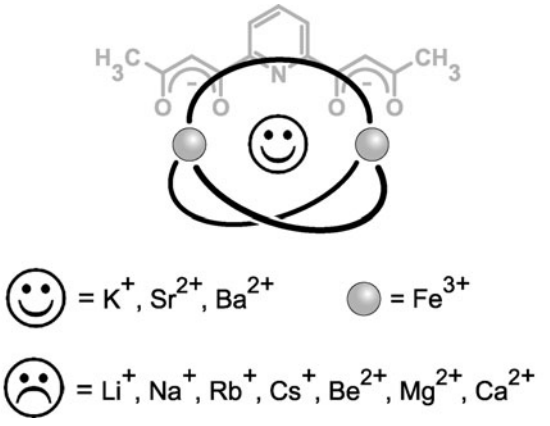

Based on density functional calculations (B3LYP/LANL2DZp (LANL2DZp=LANL2DZ augmented with polarization functions on non-hydrogen atoms)), the selectivity of the {2}-metallocryptand $[Fe_2L_3]$ (L^{2-} = 2,6-dibutane-1,3-dionylpyridine dianion) was investigated and the experimentally known K^+, Sr^{2+} and Ba^{2+} cation selectivity rationalized. The rigidity of L^{2-}, visible in the small torsion angles compared to previously investigated classical organic cryptands, can be identified as the origin of this discrimination. Derived from the hosted alkali and alkaline earth cations, the size of the {2}-metallocryptand's $[Fe_2L_3]$ cavity is analogous to the cryptand [2.2.phen]. Additionally, the quantum chemical calculations identified the {2}-metallocryptand $[Fe_2L_3]$ as the first experimentally verified metalloproton sponge (calculated (B3LYP/LANL2DZp) proton affinity −259.8 kcal mol^{-1}). This high gas-phase proton affinity clearly explains why empty $[Fe_2L_3]$ was never observed, and only $[(H^{N})_3{\subset}Fe_2L_3]^{3+}$ or $[M{\subset}Fe_2L_3]^{m+}$ are known.

Keywords: Selective ion complexation; Metallocryptands; Metallocryptates; Proton affinity; DFT

*Corresponding authors. Email: Andreas.Scheurer@fau.de (A. Scheurer); Ralph.Puchta@fau.de (R. Puchta)
For Part VI see: [1]
Dedicated to Prof. Dr. h. c. mult. Rudi van Eldik on the occasion of his 70th birthday, in appreciation of his continuous kind support and friendship.

Introduction

The quest for selective ion extraction dates back to the days of Fritz Haber and the time after the First World War [2, 3]. Today, the topic of selective ion extraction is again in focus especially in the context of recycling of the waste of nuclear power plants [4]. J.-M. Lehn made a great impact to this topic by discovering cryptand and the cryptate complexes in the late 1960s [5], leading to the Nobel prize in 1987 [6] together with D.J. Cram and C.J. Pedersen for their development and use of molecules with structure-specific interactions of high selectivity.

While Lehn and co-workers went the hard way and built up complete cage structures applying classical organic synthesis with covalent bonds, an experimentally simpler approach uses metal-directed self-assembly to build up analogous superstructures. Therefore, the concept of self-assembly allowed the synthesis of the complete family of metallotopomers to the well-known classical coronates, {2}-cryptates and {3}-cryptates (see figure 1) [7].

An absolute prerequisite for the successful application of metal-assisted self-assembly are labile structures tailor-made in the final product [8]. Such labile, often multidentate coordination sites, suitable to built up metallo-topomers, can be bis(bipyridine) [9], 8-hydroxyquinoline [10], benzimidazole derivatives [11], bis(dipyrromethene) [12], catechols [13] along with their thio derivatives [14, 15]. Saalfrank *et al.* utilized classical 1,3-diketo systems in connection with tailor-made spacers and mainly transition metal ions to construct the complete family of metallotopomers [16–32]. The most striking motivation to investigate these complexes experimentally was their selective ion complexation in connection with their bioinorganic model character for siderophores based, e.g., on rhodotorulic acid [33].

In this contribution, we will focus on the investigation of selective complexation of alkali and alkaline earth metal ions by Saalfrank-type {2}-metallocryptand leading to

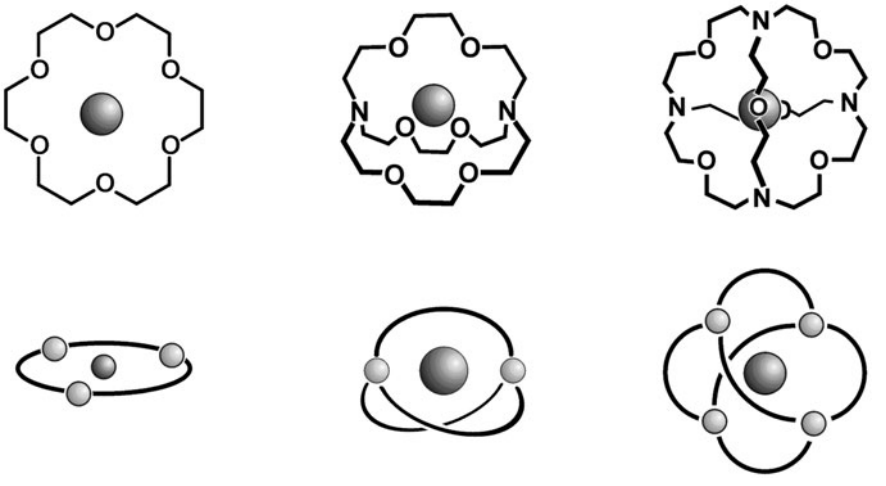

Figure 1. Classical supramolecular systems (top) and their metallotopomers (bottom; bow: ligand, balls: metal cations).

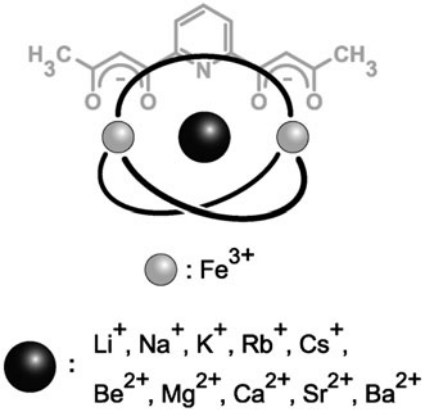

Figure 2. The QM-investigated {2}-cryptates $[M\subset Fe_2L_3]^{m+}$.

{2}-metallocryptates, formed by three deprotonated ligands L^{2-} (L^{2-} = 2,6-dibutane-1,3-dionylpyridine dianion),[†] two iron(III) ions (Fe_2L_3), and a guest cation (see figure 2).

While experimentally intensively explored, these Saalfrank-type {2}-cryptates were quantum chemically hard to handle because of their size and their paramagnetic nature [34]. Here, we present for the first time a first principle quantum chemically-based comparative study on the selective ion complexation of {2}-metallo-cryptands. As this study is not hampered by effects such as counter ions, solvent molecules, it allows an unspoiled comparison with the well-known classical Lehn cryptands and cryptates and rationalizing the experimentally observed ion selectivity in Saalfrank-type Fe_2L_3-cryptat complexes.

Quantum chemical methods

We performed hybrid density functional calculations using the B3LYP functional [35] and the LANL2DZ basis set with effective core potentials [36], augmented with polarization functions on non-hydrogen atoms [37]. The performance of this level (denoted as B3LYP/LANL2DZp) has been documented by us and others [38]. Structures were characterized as minima, transition structures, or higher order saddle points by computation of vibrational frequencies. Relative energies were corrected for zero-point vibrational energy. The stability of the wave function was tested. The GAUSSIAN suite of programs was used [39].

Results and discussion

Whereas significant data for all discussed structures are summarized in table 1, figure 3 illustrates, as a representative example, the calculated $[K\subset Fe_2L_3]^+$ complex. The crystal

[†]While for experimental reasons, terminal substituents R such as *tert*-butyl, thiophenyl, or naphthyl have been included in the ligand systems; here we restricted ourselves to the smaller methyl group.

Table 1. Calculated (B3LYP/LANL2DZp) structural and energetic data on $[M\subset Fe_2L_3]^{m+}$.

	Ionic radius (Å) [45]	$E_{complex}$ (kcal mol^{-1})	Point group	M–N (Å)	M–O (Å)	Fe–M (Å)	Fe–O_M (Å)	Fe–O (Å)	<(O–C–C–N) (°)	<(O–C···C–O) (°)
$[Li\subset Fe_2L_3]^+$	0.92	13.24	D_3 [46]	2.85	2.78	3.64	2.03	1.99	−26.0	−50.1
$[Li\subset Fe_2L_3]^+$	0.92	11.45	C_2	2.12	2.25	3.65	1.99	2.00	−14.5	27.6
				3.42	2.25		2.00	2.01	27.9	53.8
				3.42	3.11		2.01	2.09	27.9	53.8
					3.11					
					3.20					
					3.20					
$[Na\subset Fe_2L_3]^+$	1.18	−4.56	D_3	2.88	2.78	3.62	2.04	1.99	−25.5	−48.3
$[K\subset Fe_2L_3]^+$	1.51	−10.61	D_3	2.92	2.84	3.64	2.05	2.00	−27.8	−50.3
$[Rb\subset Fe_2L_3]^+$	1.61	−1.39	D_3	2.95	2.89	3.65	2.06	2.00	−29.7	−52.2
$[Cs\subset Fe_2L_3]^+$	1.74	17.72	D_3	3.01	2.96	3.67	2.09	2.00	−32.5	−55.0
$[Be\subset Fe_2L_3]^{2+}$	0.45	−20.63	C_1	1.87	1.61	3.48	1.85	1.86	−3.7	−21.7
				3.02	1.61	4.32	1.89	1.89	−9.8	7.6
				3.44	1.75		2.02	1.96	−10.0	14.9
					2.82		2.24	1.97	−12.7	
					3.43		3.23	2.04	22.7	
					4.00		3.50	2.04	26.5	
$[Mg\subset Fe_2L_3]^{2+}$	0.89	−14.37	D_3	2.67	2.39	3.34	2.05	2.00	2.16	−3.9
$[Ca\subset Fe_2L_3]^{2+}$	1.12	−46.03	D_3	2.91	2.63	3.58	2.06	1.98	−12.9	−26.1
$[Sr\subset Fe_2L_3]^{2+}$	1.26	−51.71	D_3	2.92	2.72	3.63	2.07	1.98	−17.8	−34.8
$[Ba\subset Fe_2L_3]^{2+}$	1.42	−49.25	D_3	2.95	2.80	3.67	2.08	1.98	−22.4	−39.9
Fe_2L_3	–	–	C_1	–	–	–	2.02	2.02	−36.1	−66.1
							2.02	2.02	−36.4	−66.8
							2.02	2.02	−36.7	−66.8
							2.02	2.02		
							2.01	2.02		
							2.01	2.02		
$[(H^N)\subset Fe_2L_3]^+$	–	–	C_2	1.03	2.24	4.07	1.98	1.99	20.3	41.4
				4.29	3.91		1.99	2.02	31.8	60.7
				4.29	3.97		2.09	2.05	34.2	60.7

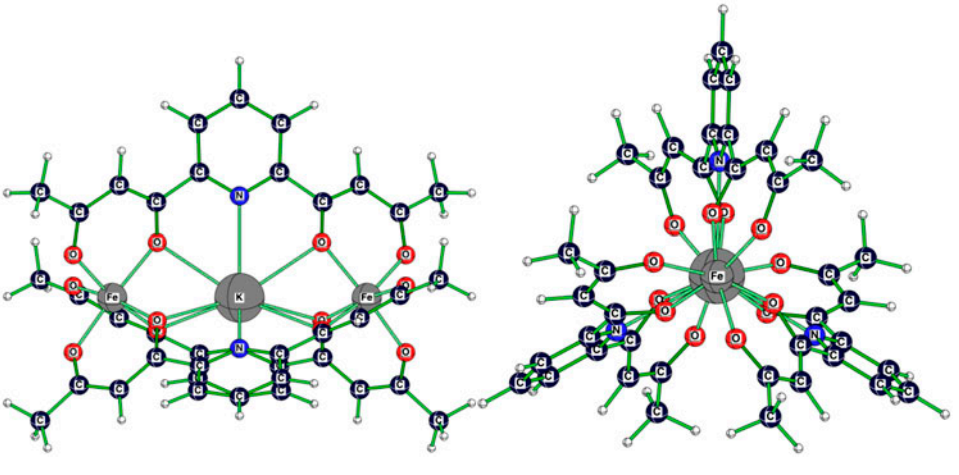

Figure 3. Calculated (B3LYP/LANL2DZp) structure (D_3) for $[K\subset Fe_2L_3]^+$.

Table 2. Overview of published crystal structure data of $[M\subset Fe_2L_3]^{m+}$ and $[(H^N)_3\subset Fe_2L_3]^{3+}$.

	Group *R*	CSD-Ref. code	M–N (Å)	M–O (Å)	Fe–M (Å)	Fe–O_M (Å)	Fe–O (Å)	<(O–C–C–N) (°)	<(O–C···C–O) (°)
$[K\subset Fe_2L_3]^+$	*t*Bu	NEXHAZ	2.89	2.78	3.57	2.00	2.00	32.0	4.3
		[29]	2.88	2.78	3.58	2.00	1.99	29.6	1.9
			2.57	2.79		2.00	1.99	29.3	2.3
				2.80		2.00	1.98	−29.8	
				2.81		2.01	1.98	−31.7	
				2.81		2.01	1.98	−31.9	
	Thio	XESJOU	2.88	2.80	3.51	1.99	1.99	−34.4	−44.1
		[30]	2.91	2.68	3.50	2.02	1.97	−9.6	−42.3
			2.96	2.85		2.01	1.98	−26.9	−35.8
				1.99		2.00	2.00	−21.5	
				2.00		2.00	1.99	−11.2	
				2.00		1.99	1.98	−29.0	
	Naph	XESKEL	2.86	2.82	3.61	2.04	1.98	−33.5	−41.1
		[30]	2.86	2.82	3.60	2.04	1.98	−15.2	−41.1
			2.86	2.82		2.04	1.98	−33.5	−41.1
				2.80		2.03	1.99	−15.2	
				2.80		2.03	2.00	−33.5	
				2.80		2.03	2.00	−15.2	
$[(H_2O)\cdot Sr\subset Fe_2L_3]^{2+}$	*t*Bu	FABQII	2.84	2.60	3.57	2.03	1.96	22.7	44.2
		[31]	2.78	2.74	3.59	2.02	1.96	22.4	40.9
			3.02	2.75		2.01	1.97	3.3	12.9
				2.67		2.02	1.98	27.2	
				2.61		2.02	1.97	19.9	
				2.94		2.01	1.97	14.2	
$[(H_2O)\cdot Sr\subset Fe_2L_3]^{2+}$	*t*Bu	LOFREE	2.91	2.69	3.58	2.02	1.97	3.3	44.2
		[32]	2.95	2.68	3.59	2.02	1.97	14.2	40.9
			2.77	2.69		2.01	1.98	19.9	12.9
				2.74		2.00	1.96	22.7	
				2.74		2.02	1.96	22.4	
				2.60		2.03	1.97	27.2	
$[(THF)_2Ba\subset Fe_2L_3]^{2+}$	*t*Bu	XESJUA	2.91	2.74	3.58	2.03	1.96	24.3	45.7
		[30]	2.89	2.75	3.60	2.01	1.97	25.6	42.2
			2.88	2.78	3.58	2.01	1.98	16.9	34.6
			2.94	2.72	3.60	2.01	1.95	29.1	−39.1
			2.84	2.75		2.02	1.97	26.6	−37.9
			2.89	2.80		2.04	1.98	12.4	−48.7
				2.67		2.04	1.96	−12.7	
				2.73		2.04	1.98	−30.6	
				2.84		2.00	1.98	−17.5	
				2.73		2.00	1.97	−25.0	
				2.75		2.01	1.97	−33.9	
				2.89		2.01	1.96	−20.7	
$[(H^N)_3\subset Fe_2L_3]^{3+}$ [M->H]	*t*Bu	FABQOO	3.89	2.14	3.90	2.00	2.00	16.4	26.6
		[29]	3.91	2.12	3.86	1.98	1.98	10.8	19.2
			3.87	2.16	3.90	1.98	2.00	10.3	29.5
			3.87	2.07	3.83	1.98	2.01	6.7	18.0
			3.84	2.11	3.96	1.97	2.00	13.4	25.4
			3.88	2.10	3.78	1.97	2.01	14.6	33.6
			3.90	2.16	3.90	1.98	1.97	12.0	
			3.90	2.09	3.87	1.99	2.01	4.8	
			3.78	2.11	3.91	1.95	2.01	6.3	
			3.86	2.10	3.84	1.98	2.04	16.0	
			3.83	2.13	3.87	1.95	2.00	16.5	
			3.96	2.11	3.88	1.99	2.01	13.5	

Notes: M- > H: For this structure, the M–O, M–N, and M–Fe distances should be understood as H_{Py}–O, H_{Py}–N, and H_{Py}–Fe distances.

structures of the potassium, strontium, and barium ion containing metallocryptates were generated by Saalfrank's group, and the key parameters are given in table 2. Although the three strands (ligands) of the experimentally investigated supramolecular structures contain much larger substituents R (*tert*-butyl, 1-naphthyl (Naph), thiophenyl (Thio)), the structural data resemble our calculated parameters. This is evidence that the selected method (B3LYP/LANL2DZp) is applicable to study the selectivity of the chosen metallocryptand (Fe_2L_3), as it was already applied to different series of classical cryptands [1, 40–44].

As shown in earlier contributions, two properties, viz. bond distances and energies of model reactions, have proven to be the basic concept for the prediction of a favorable and selective ion complexation. Comparison of the bond distances between the donor atoms and the endohedrally encapsulated metal cation in the metallocryptand, on one hand, and the coordination by solvent molecules, e.g., pyridine or water, on the other hand, can be drawn. This method is valid if the donor atoms coordinating to the metal ions are the same, as well as equally or at least similarly hybridized in the cryptand and the reference system. Therefore, we compare the distances obtained in this work with $[M(pyridine)_n]^{m+}$ and $[M(H_2O)_n]^{m+}$ (n = 4 for Li^+ and Be^{2+} and 6 for all others), see figures 4 and 5. The bisecting lines in the figures represent the cases in which coordination will most likely occur. The ions above the line are somehow too small, whereas the ions below the line are too large for the studied macromolecular cages.

The Be^{2+} and Li^+ ions seem to be too small for the studied metallocryptands. Whereas the calculated D_3 structure of $[Li\subset Fe_2L_3]^+$ is a higher order saddle point, no D_3 structure of $[Be\subset Fe_2L_3]^{2+}$ could be determined. Local minima on the potential hypersurface can be obtained for both systems upon lowering the symmetry, C_1 for $[Be\subset Fe_2L_3]^{2+}$ and C_2 for $[Li\subset Fe_2L_3]^+$, respectively. Figures 4 and 5 reveal that the interaction with both types of donors, nitrogen and oxygen, are important for these small cations. Since they are too small for the cavity, they are shifted toward one of the ligand strands and coordinate to the pyridine nitrogen and three oxygen atoms. This fact is reflected by the very different metal

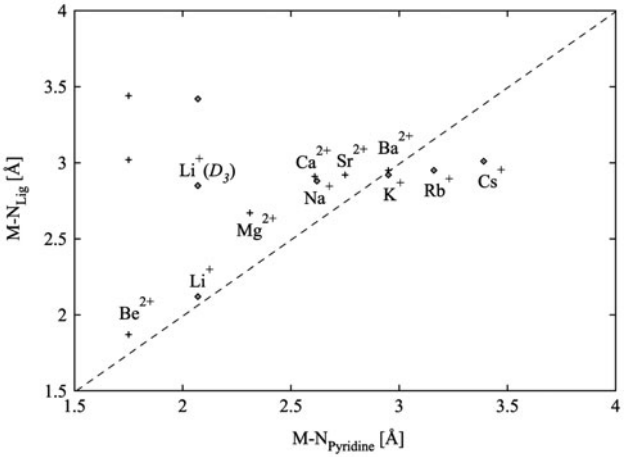

Figure 4. Calculated (B3LYP/LANL2DZp) M–N-distance in $[M\subset Fe_2L_3]^{m+}$ plotted against the calculated (B3LYP/LANL2DZp) M–N-distance in $[M(pyridine)_n]^{m+}$ (n = 4 in case of Li^+ and Be^{2+}, n = 6 in all other cases) [44].

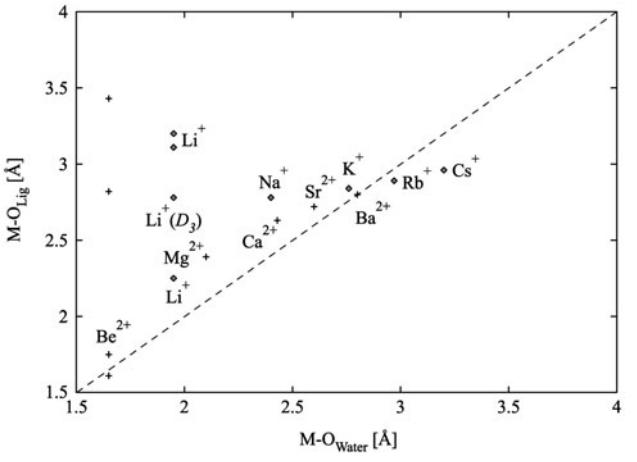

Figure 5. Calculated (B3LYP/LANL2DZp) M–O-distance in $[M\subset Fe_2L_3]^{m+}$ plotted against the calculated (B3LYP/LANL2DZp) M–O-distance in $[M(OH_2)_n]^{m+}$ (n = 4 in case of Li^+ and Be^{2+}, n = 6 in all other cases) [44].

ion–donor atom distances, see table 1. This is logical, since beryllium and lithium usually prefer a coordination number of four.

In contrast, we could determine the D_3 structure of $[Mg\subset Fe_2L_3]^{2+}$ by our DFT calculations; however, the magnesium cation is quite small and therefore lies far above the bisecting line in both plots, pointing to weak stabilization for this metal dication by the studied supramolecule. The structures of $[Rb\subset Fe_2L_3]^{+}$ and $[Cs\subset Fe_2L_3]^{+}$ demonstrate a comparable situation, but the other way round. These large cations prefer higher coordination numbers but are obviously too large for the studied cavity, sitting below the bisecting line in both plots.

For the remaining metal ions, the interaction with all donors seems to be necessary, as shown in figures 4 and 5. For three of them (Sr^{2+}, K^+, and Ba^{2+}), ion exchange experiments in solution and solid state were done in cooperation by the research teams of R.W. Saalfrank and B. Roling [32, 47, 48]. These experiments demonstrated that the strontium dication can be replaced by a potassium monocation in the cavity of the metallocryptand, whereas the barium and potassium cations stay encapsulated inside the supramolecule. It was concluded that the size of the guest cations relative to the size of the {2}-cryptand's cavity determines how strong the guest cations are bound. This experimental finding is in agreement with our results: while K^+ and Ba^{2+} are sitting exactly on the bisecting line, Sr^{2+} is located slightly above it.

According to the performed comparison of the bond lengths between metal cations and N/O donor atoms in cryptates, with the same bond lengths of the solvated metal centers, the following conclusion can be drawn: Sr^{2+}, K^+, and Ba^{2+} fit best into the cavity, undergoing relevant interactions with all donor atoms. These results resemble those obtained experimentally, where diironcryptates of the same cations show high coordination numbers in the isolated crystal structures.

Besides the structural evaluation of the computed systems, examination of energies based on the model reaction (1) also provides significant and important information for prediction of the selectivity of the studied {2}-cages. For the sake of consistency, all cations were calculated in a sixfold coordination environment. Though the lithium and beryllium cations

prefer fourfold coordination and corresponding structures were actually found [49, 50], the gas-phase species $[Li(H_2O)_6]^+$ and $[Be(H_2O)_6]^{2+}$ exist as local minima [1, 44]. The complexation energies calculated in this way are shown in table 1 and are plotted against the ionic radii in figure 6.

$$[M(H_2O)_6]^{m+} + [Fe_2L_3] \rightarrow [M \subset Fe_2L_3]^{m+} + 6\ H_2O \quad (1)$$

According to our calculations, the most unfavorable values of the complexation energy among the alkali cations present the structures of lithium and cesium. The large positive values are linked to the poor matching inside the diironcryptand of both ions, one being too small and the other too large for the cavity. For the remaining alkali metals, negative complexation energies were found, revealing the potassium derivative as the most stable complex $[K\subset Fe_2L_3]^+$ with an endohedral guest followed by sodium $[Na\subset Fe_2L_3]^+$. The value for $[Rb\subset Fe_2L_3]^+$ is negative but in fact very small pointing to insufficient encapsulation of this ion as well due to its size.

All studied alkaline earth cations demonstrate negative complexation energies due to their dicationic nature and the extra stabilization of the charge in the large supramolecule. The smallest values were found for beryllium and magnesium, since both cations are too small for the appropriate coordination inside the metallocryptand. The lowest value was found for $[Sr\subset Fe_2L_3]^{2+}$ followed by $[Ba\subset Fe_2L_3]^{2+}$ and $[Ca\subset Fe_2L_3]^{2+}$. These ions seem to fit well into the cavity, indicated by a significant decrease in energy values.

In general, the energy consideration confirms our prediction made by the evaluation of the structural parameters. The smaller (Li^+, Be^{2+}, and Mg^{2+}) and the larger (Rb^+ and Cs^+) cations do not fit well in the available cavity. Although the calculated structures allow appropriate coordination and stabilization in the gas phase, in solution, these structures will surely not be superior to solvated cations and an empty metallocryptand.

The observed preference for the cation size can be correlated with the cavity size and, hence, with the selectivity of the cryptand. Thereby, the preferred selectivity of the alkaline

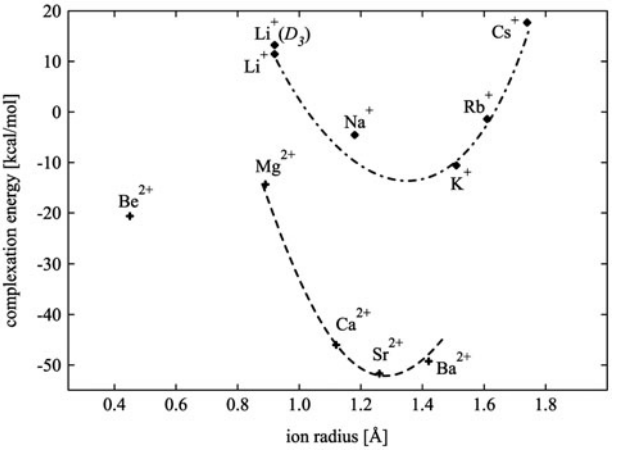

Figure 6. Calculated (B3LYP/LANL2DZp) complexation energy for $[M\subset Fe_2L_3]^{m+}$ according to equation 1, plotted against the ionic radius of M^{m+} [45].

earth ions plays a more important role, since alkali cations are not very sensitive in this range, as the ion radius difference for Li^+, Na^+, and K^+ is too large. An overview of the preferred ion selectivity of several cryptand families studied by our group was published recently [44]. A comparison of these data with the current results demonstrates that the cavity size of the investigated diironcryptand is very similar to the cavity in [2.2.phen] [43]. This is an interesting observation, as (i) the flexibility and the nature of the bars forming the cage are very different and (ii) the number and the hybridization of the donor atoms vary. While in $[Fe_2L_3]$, three equal, but only moderately flexible ligands form the cage, in [2.2.phen], one restricted (phenanthroline) and two more loose (diether) molecular bars build up the {2}-cryptand. The number of the donors differs by one. In [2.2.phen], eight donors (two sp^2-N-, two sp^3-N-, and four sp^3-O) are provided to nest the guest. In contrast, we have nine donors (three sp^2-N- and six formally sp^2-O) for the endohedral coordination of the metal ion in $[Fe_2L_3]$. A particular feature of the O-donors has to be mentioned: six of the acetylacetonate oxygen donors are not only involved in the binding of the guest ions, they are responsible for the formation of the {2}-cryptand by coordinating the bridge-head Fe^{3+} ions, too. This behavior of acetylacetonate's carbonyl oxygens as ligands for two metal ions is also observed without the necessity of the formation of cages and the inclusion of ions inside. Examples are reported by the research teams of Döring, Brodersen, Dahlenburg, and others [51, 52].

The former articles of our [1, 41–44] and other [53] groups demonstrate that the cryptand does not remain unaltered throughout the complexation: it twists in order to adjust for the optimal interaction with the metal guest cation. A comparison of the calculated distances (see table 1) shows a general increase in the metal–donor bond lengths with increasing size of the guest ions. Apart from various contributions of the guest ions, the observed behavior is evidence for the flexibility of the studied metallocryptand. Descriptors for this flexibility are the torsion angles O–C···C–O and O–C–C–N. They show a qualitatively linear behavior that mainly depends on the size of the ion, see figures 7 and 8, respectively.

Since the small cations (Li^+ and Be^{2+}) are too small for the investigated metallo-cryptand and are shifted sideways in the cavity, their values are omitted of the presented trends.

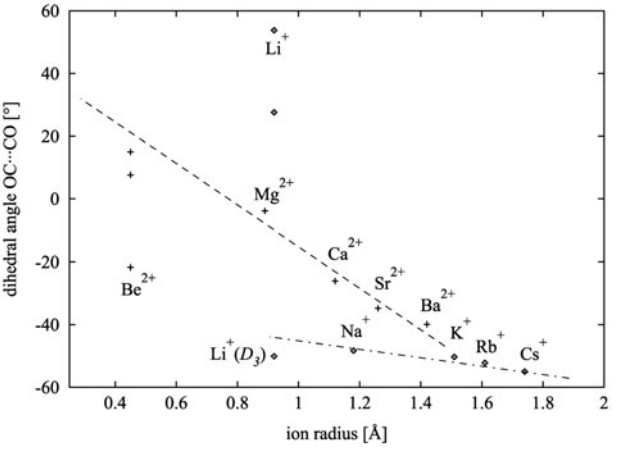

Figure 7. Calculated (B3LYP/LANL2DZp) dihedral angle O–C···C–O of L^{2-} in $[M\subset Fe_2L_3]^{m+}$ plotted against the ionic radius of M^{m+} [45].

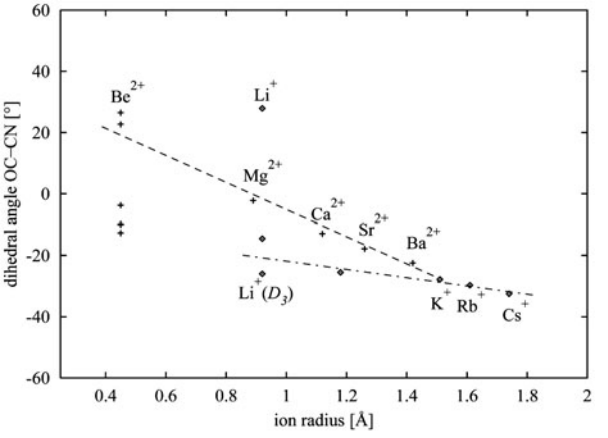

Figure 8. Calculated (B3LYP/LANL2DZp) dihedral angle OC–CN of L^{2-} in $[M\subset Fe_2L_3]^{m+}$ plotted against the ionic radius of M^{m+} [45].

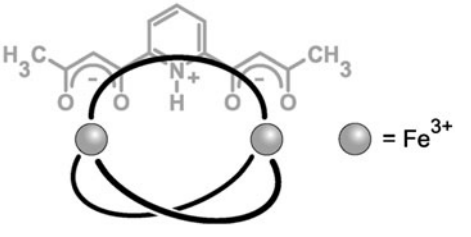

Figure 9. The investigated {2}-cryptand $[Fe_2L_3]$ in protonated form $[(H^N)_3\subset Fe_2L_3]^{3+}$.

Whereas the studied torsion angles cover similarly small ranges in the case of alkali cations, 7.0° and 6.7° for O–C–C–N and O–C···C–O, respectively, earth alkaline metal ions demonstrate notable differences: 9.5°[†] and 36.0° for O–C–C–N and O–C···C–O, respectively. The larger value indicates that the twist of the pyridine moiety along the C_2 axis of the molecule is more important for the mutual adjustment of the diironcryptand and alkaline earth metals. Both angles increase with the increasing size of the cations and are negative, except for the O–C–C–N angle in $[Mg\subset Fe_2L_3]^{2+}$. Therefore, the stereochemistry of the cage is λ [42]. We take this as a further indication that the Mg^{2+} ion, smaller than the Li^+ ion, should be interpreted as a borderline case, where the smaller ion size is compensated by the attraction of the dicationic charge supporting the formation of the calculated D_3 metallocryptand.

Summing up the above presented quantum chemical results and comparing them with our previous quantum chemical findings for classical Lehn-type cryptands [44], we see total agreement with the experimental results of the R.W. Saalfrank research team and can easily rationalize them. While the classical Lehn cryptands are relatively flexible, as the larger twist angles of the coordinating chains show, the Saalfrank-type metallo-topomers are rigid.

[†]The $[Mg\subset Fe_2L_3]^{2+}$ O-C-C-N value is not included, as it could be addressed as a special case. *Vide supra*.

Therefore, they show higher ion selectivity and will only bind K^+, Sr^{2+}, and Ba^{2+} as guests in $[Fe_2L_3]$. The quantum chemical investigations of the Saalfrank-type {2}-cryptand $[Fe_2L_3]$ allow understanding why experimentally only the three-time protonated form of $[Fe_2L_3]$, namely $[(H^N)_3{\subset}Fe_2L_3]^{3+}$, is accessible, if no suitable metal ions for complexation are available (figure 9).

As shown in table 3, the calculated gas-phase proton affinity of all {2}-cryptands is in the range of the traditional proton sponge 1,8-bis(dimethylamino)naphthalene and the first natural occurring proton sponge Porphyra-334 [55]. Of course, a direct 1:1 comparison of the gas-phase proton affinity between $[Fe_2L_3]$ and the classical pure organic proton sponges is difficult and already hampered by the molecules' size and the molecular mechanisms giving the high gas-phase proton affinities. While in Porphyra-334, the positive charge can be distributed over a large part of the molecule; in 1,8-bis(dimethylamino)naphthalene, the strain of the two $(CH_3)_2N$-nitrogen lone pairs pointing to each other is responsible for the high experimental basicity, here approximated as high gas-phase proton affinity. The identical situation is present in the cage of the listed {2}-cryptands. While in 1,8-bis(dimethylamino)naphthalene and Porphyra-334 nitrogens are exclusively responsible for the high observed values, in [1.1.1], [2.2.2], [2.2.phen], and the {2}-metallocryptands $[Pd_3L^2_2]$ and $[Fe_2L_3]$ lone pairs of oxygens and nitrogens are the origins of the increased electron density inside the cavity. As expected in all cases, nitrogens are the preferred proton acceptors.

Calculated gas-phase proton affinity is of course a simple and crude descriptor for the experimental basicity in solutions, as important contributions of basicity are neglected. Taking these limitations into account, we see indications that the investigated Saalfrank-type cryptand can be understood as the first experimentally known metallocryptand that can be interpreted as a metalloproton sponge-based on our calculated gas-phase proton affinity of -259.8 kcal mol^{-1}. Since in solution and solid-state investigations, counterions and solvents are present and stabilize the positive charge of the cage compound, three protons can be hosted. In our gas-phase calculations, the addition of a second and third positive charge would be unfavorable due to the Coulomb repulsion. Additionally, these gas-phase proton affinity data are in agreement with the experimental observation, that $[(H^N)_3{\subset}Fe_2L_3]^{3+}$ cannot be deprotonated by 1,8-bis(dimethylamino)naphthalene during experimental investigations in solution [47, 48].

Table 3. Calculated (B3LYP/LANL2DZp) gas-phase proton affinities for selected bases and {2}-cryptands.

	Proton affinity (exp.) [54] (kcal mol^{-1})	Proton affinity (RB3LYP/LANL2DZp) (kcal mol^{-1})
NH_3	−202.3	−206.0
Pyridine	−219.9	−222.1
1,8-bis (dimethylamino)naphthalene	−241.5	−247.3
$N(CH_3)_3$	−224.8	−226.5
2,6-Diacetylpyridine	–	−219.8
Porphyra-334 [55]	–	$-265.7^{[6-31G^*]}$
$[H{\subset}1.1.1]^+$ [56]	–	−251.8
$[H{\subset}2.2.2]^+$ [56]	–	−254.4
$[H{\subset}2.2.phen]^+$	–	−251.5
$[H{\subset}Pd_3L^2_2]^+$ [57][a]	–	−257.1
$[H{\subset}Fe_2L_3]^+$	–	−259.8

[6−31G*] Calculated by B3LYP/6−31G*

[a]The cryptand $[Pd_3L^2_2]$ [$(L^2)^{3-}$: 1,1′,1″-nitrilotris(5,5-dimethylhexane-2,4-dione trianion)] is the first quantum chemically suggested metalloproton sponge, derived from [2.2.2], following the concept of metallotopomers.

Summary

We were able to show by DFT (B3LYP/LANL2DZp) calculations that the {2}-metallocryptand family [Fe_2L_3] can host K^+, Sr^{2+}, and Ba^{2+} cations in accordance with previous experiments. We attribute this to the rigidity of the three L^{2-} ligands (2,6-dibutane-1,3-dionylpyridine dianion) forming with two iron-(III)-cations the {2}-cryptand [Fe_2L_3]. According to the hosted alkali and alkaline earth cations, the cavity size of the Saalfrank-type {2}-metallocryptands [Fe_2L_3] is comparable to the one found in Lehn-type cryptand [2.2.phen]. Based on calculated gas-phase proton affinities, the {2}-metallocryptands [Fe_2L_3] show outstanding proton affinity and can be understood as the first experimentally verified system being a metalloproton sponge. This explains the experimental observation, too, that up to now, no unprotonated and completely empty system [Fe_2L_3] was accessible.

Acknowledgments

A.S. and R.P. acknowledge the continuous manifold support of Prof. Dr. Rolf W. Saalfrank through all the years and his endorsement to perform this research program. Additionally, we thank Prof. Tim Clark for hosting this work at the CCC and the Regionales Rechenzentrum Erlangen (RRZE) for a generous allotment of computer time.

Disclosure statement

No potential conflict of interest was reported by the authors.

ORCID

Andreas Scheurer http://orcid.org/0000-0002-2858-9406
Ralph Puchta http://orcid.org/0000-0003-1370-3875

References

[1] S. Begel, R. Puchta, R. van Eldik. *J. Mol. Model.*, **20**, 2200 (2014).
[2] F. Haber. *Angew. Chem.*, **40**, 303 (1927).
[3] R. Hahn. *Gold aus dem Meer: Die Forschungen des Nobelpreistragers Fritz Haber in den Jahren 1922–1927*, GNT Verlag, Berlin (1999).
[4] see exemplarily: (a) V. Amendola, G. Bergamaschi, M. Boiocchi, R. Albertoc, H. Braband. *Chem. Sci.*, **5**, 1820 (2014); (b) P. Maciejewski, M. Żuber, M. Ulewicz, K. Sobianowska. *Physicochem. Prob. Miner. Process.*, **43**, 65 (2009); (c) P. Maciejewski, W. Walkowiak. *Physicochem. Prob. Miner. Process.*, **38**, 139 (2004); (d) R.M. Izait, K. Pawlak, J.S. Bradshaw. *Chem. Rev.*, **91**, 1721 (1991); (e) P. Fux, J. Lagrange, P. Lagrange. *J. Chim. Phys.*, **81**, 321 (1984).
[5] (a) B. Dietrich, J.-M. Lehn, J.P. Sauvage. *Tetrahedron Lett.*, **10**, 2885 (1969); (b) B. Dietrich, J.-M. Lehn, J.P. Sauvage. *Tetrahedron Lett.*, **10**, 2889 (1969).
[6] J.-M. Lehn. *Angew. Chem.*, **100**, 91 (1988); *Angew. Chem. Int. Ed. Eng.*, **27**, 89 (1988).
[7] E. Uller, B. Demleitner, I. Bernt, R.W. Saalfrank. In *Structure and Bonding*, M. Fujita (Eds), Vol. 96, p. 149–175, Springer, Berlin (2000).
[8] (a) R. Brachvogel, F. Hampel, M. von Delius. *Nat. Commun.*, **6** (2015). doi:10.1038/ncomms8129. (b) R. Brachvogel, M. von Delius. *Chem. Sci.*, **6**, 1399 (2015).
[9] See e.g. (a) B.R. Serr, K.A. Andersen, C.M. Elliott, O.P. Anderson. *Inorg. Chem.*, **27**, 4499 (1988); (b) M.-T. Youinou, R. Ziessel, J.-M. Lehn. *Inorg. Chem.*, **30**, 2144 (1991); (c) C.M. Elliott, D.L. Derr, S. Ferrere, M.D.

Newton, Y.-P. Liu. *J. Am. Chem. Soc.*, **118**, 5221 (1996); (d) M. Albrecht, C. Riether. *Chem. Ber.*, **129**, 829 (1996); (e) S. Goetz, P.E. Kruger. *Dalton Trans.*, **34**, 1277 (2006) and literature cited therein.
[10] See e.g. (a) M. Albrecht, O. Osetska. *Eur. J. Inorg. Chem.*, 4678 (2010); (b) M. Albrecht, O. Osetska, J.-C.G. Bünzli, F. Gumy, R. Fröhlich. *Chem. Eur. J.*, **15**, 8791 (2009); (c) M. Albrecht, O. Blau, J. Zauner. *Eur. J. Org. Chem.*, 3165 (1999); (d) M. Albrecht, O. Blau, R. Fröhlich. *Chem. Eur. J.*, **5**, 48 (1999); (e) M. Albrecht, O. Blau. *Chem. Commun.*, 345 (1997) and literature cited therein.
[11] See e.g. (a) A.F. Williams, C. Piguet, G. Bernardinelli. *Angew. Chem.*, **103**, 1530 (1991); *Angew. Chem., Int. Ed. Eng.*, **30**, 1490 (1991); (b) L.J. Charbonniere, G. Bernardinelli, C. Piguet, A.M. Sargeson, A.F. Williams. *J. Chem. Soc., Chem. Commun.*, 1419 (1994); (c) L.J. Charbonniere, A.F. Williams, U. Frey, A.E. Merbach, P. Kamalaprija, O. Schaad. *J. Am. Chem. Soc.*, **119**, 2488 (1997) and literature cited therein.
[12] See e.g. Z. Zhang, D. Dolphin. *Chem. Commun.*, 6931 (2009) and literature cited therein.
[13] See e.g. (a) M. Albrecht, S. Burk, R. Stoffel, A.A. Lüchow, R. Fröhlich, M. Kogej, C.A. Schalley. *Eur. J. Inorg. Chem.*, 1361 (2007); (b) I. Janser, M. Albrecht, K. Hunger, S. Burk, K. Rissanen. *Eur. J. Inorg. Chem.*, 244 (2006); (c) M. Albrecht, S. Kotila. *Angew. Chem.*, **107**, 2285 (1995); *Angew. Chem. Int. Ed. Eng.*, **34**, 2134 (1995) and literature cited therein.
[14] See e.g. (a) F. Hupka, F.E. Hahn. *Chem. Commun.*, **46**, 3744 (2010); (b) F.E. Hahn, B. Birkmann, T. Pape. *Dalton Trans.*, 2100 (2008); (c) F.E. Hahn, T. Kreickmann, T. Pape. *Dalton Trans.*, 769 (2006); (d) T. Kreickmann, C. Diedrich, T. Pape, H.V. Huynh, S. Grimme, F.E. Hahn. *J. Am. Chem. Soc.*, **128**, 11808 (2006) and literature cited therein.
[15] For a review see: M. Albrecht. *Chem. Rev.*, **101**, 3457 (2001).
[16] R.W. Saalfrank, A. Scheurer, R. Puchta, F. Hampel, H. Maid, F.W. Heinemann. *Angew. Chem.*, **119**, 269 (2007); *Angew. Chem. Int. Ed.*, **46**, 265 (2007).
[17] R.W. Saalfrank, N. Mooren, A. Scheurer, H. Maid, F.W. Heinemann, F. Hampel, W. Bauer. *Eur. J. Inorg. Chem.*, 4815 (2007).
[18] O.E. Woisetschläger, A. Scheurer, R.W. Saalfrank, W. Beck. *Z. Anorg. Allg. Chem.*, **633**, 2141 (2007).
[19] R.W. Saalfrank, C. Spitzlei, A. Scheurer, H. Maid, F.W. Heinemann, F. Hampel. *Chem. Eur. J.*, **14**, 1472 (2008).
[20] R.W. Saalfrank, H. Maid, A. Scheurer. *Angew. Chem.*, **120**, 8924 (2008); *Angew. Chem. Int. Ed.*, **47**, 8794 (2008).
[21] R.W. Saalfrank, H. Maid, A. Scheurer, F.W. Heinemann, R. Puchta, W. Bauer, D. Stern, D. Stalke. *Angew. Chem.*, **120**, 9073 (2008); *Angew. Chem. Int. Ed.*, **47**, 8941 (2008).
[22] R.W. Saalfrank, H. Maid, A. Scheurer, R. Puchta, W. Bauer. *Eur. J. Inorg. Chem.*, 2903 (2010).
[23] R.W. Saalfrank, A. Scheurer. *Top. Curr. Chem.*, **319**, 125 (2012).
[24] H. Maid, F.W. Heinemann, A. Scheurer, N. Mooren, R.W. Saalfrank, W. Bauer. *Helv. Chim. Acta*, **95**, 2429 (2012).
[25] R.W. Saalfrank, A. Breit, A. Dresel, S. Trummer, A. Welch, A.X. Trautwein, E. Bill. *J. Inorg. Biochem.*, **59**, 101 (1995).
[26] R.W. Saalfrank, N. Löw, F. Hampel, H.-D. Stachel. *Angew. Chem.*, **108**, 2353 (1996); *Angew. Chem. Int. Ed. Eng.*, **35**, 2209 (1996).
[27] R.W. Saalfrank, N. Löw, B. Demleitner, D. Stalke, M. Teichert. *Chem. Eur. J.*, **4**, 1305 (1998).
[28] R.W. Saalfrank, N. Löw, S. Kareth, V. Seitz, F. Hampel, D. Stalke, M. Teichert. *Angew. Chem.*, **110**, 182 (1998); *Angew. Chem. Int. Ed.*, **37**, 172 (1998).
[29] R.W. Saalfrank, A. Dresel, V. Seitz, S. Trummer, F. Hampel, M. Teichert, D. Stalke, C. Stadler, J. Daub, V. Schünemann, A.X. Trautwein. *Chem. Eur. J.*, **3**, 2058 (1997).
[30] R.W. Saalfrank, V. Seitz, F.W. Heinemann, C. Göbel, R. Herbst-Irmer. *J. Chem. Soc., Dalton Trans.*, 599 (2001).
[31] R.W. Saalfrank, V. Seitz, D.L. Caulder, K.N. Raymond, M. Teichert, D. Stalke. *Eur. J. Inorg. Chem.*, 1313 (1998).
[32] R. Puchta, B. Roling, A. Scheurer, V. Weiskopf, F. Hampel, N.J.R. van Eikema Hommes, H.-U. Hummel. *Solid State Ionics*, **179**, 489 (2008).
[33] C.J. Carrano, K.N. Raymond. *J. Am. Chem. Soc.*, **100**, 5371 (1978).
[34] R. Puchta, V. Seitz, N.J.R. van Eikema Hommes, H.-U. Hummel. *J. Mol. Model.*, **6**, 126 (2000).
[35] (a) A.D. Becke. *J. Phys. Chem.*, **97**, 5648 (1993); (b) C. Lee, W. Yang, R.G. Parr. *Phys. Rev. B: Condens. Matter*, **37**, 785 (1988); (c) P.J. Stephens, F.J. Devlin, C.F. Chabalowski, M.J. Frisch. *J. Phys. Chem.*, **98**, 11623 (1994).
[36] (a) T.H. Dunning Jr., P.J. Hay. In *Modern Theoretical Chemistry: Methods of Electronic Structure Theory*, H.F. Schaefer III (Ed.), Chap. 1, Vol. 3, pp. 1–30, Plenum, New York (1977); (b) P.J. Hay, W.R. Wadt. *J. Chem. Phys.*, **82**, 270 (1985); (c) P.J. Hay, W.R. Wadt. *J. Chem. Phys.*, **82**, 284 (1985); (d) P.J. Hay, W.R. Wadt. *J. Chem. Phys.*, **82**, 299 (1985).
[37] S. Huzinaga (Ed.). *Gaussian Basis Sets for Molecular Calculations*, Elsevier, Amsterdam (1984).
[38] See e.g. (a) S. Klaus, H. Neumann, H. Jiao, A. Jacobi von Wangelin, D. Gördes, D. Strübing, S. Hübner, M. Hately, C. Weckbecker, K. Huthmacher, T. Riermeier, M. Beller. *J. Organomet. Chem.*, **689**, 3685 (2004); (b) R.W. Saalfrank, C. Deutscher, H. Maid, A.M. Ako, S. Sperner, T. Nakajima, W. Bauer, F. Hampel, B.A. Heß,

N.J.R. van Eikema Hommes, R. Puchta, F.W. Heinemann. *Chem. Eur. J.*, **10**, 1899 (2004); (c) P. Illner, A. Zahl, R. Puchta, N.J.R. van Eikema Hommes, P. Wasserscheid, R. van Eldik. *J. Organomet. Chem.*, **690**, 3567 (2005); (d) A. Scheurer, H. Maid, F. Hampel, R.W. Saalfrank, L. Toupet, P. Mosset, R. Puchta, N.J.R. van Eikema Hommes. *Eur. J. Org. Chem.*, 2566 (2005); (e) A. Scheurer, R. Puchta, F. Hampel. *J. Coord. Chem.*, **63**, 2868 (2010); (f) M. Walther, B.M. Alzubi, R. Puchta, G. Linti, R. Meier, R. van Eldik. *J. Coord. Chem.*, **64**, 18 (2011) and references cited therein.

[39] M.J. Frisch, G.W. Trucks, H.B. Schlegel, G.E. Scuseria, M.A. Robb, J.R. Cheeseman, J.A. Montgomery Jr., T. Vreven, K.N. Kudin, J.C. Burant, J.M. Millam, S.S. Iyengar, J. Tomasi, V. Barone, B. Mennucci, M. Cossi, G. Scalmani, N. Rega, G.A. Petersson, H. Nakatsuji, M. Hada, M. Ehara, K. Toyota, R. Fukuda, J. Hasegawa, M. Ishida, T. Nakajima, Y. Honda, O. Kitao, H. Nakai, M. Klene, X. Li, J.E. Knox, H.P. Hratchian, J.B. Cross, V. Bakken, C. Adamo, J. Jaramillo, R. Gomperts, R.E. Stratmann, O. Yazyev, A.J. Austin, R. Cammi, C. Pomelli, J.W. Ochterski, P.Y. Ayala, K. Morokuma, G.A. Voth, P. Salvador, J.J. Dannenberg, V.G. Zakrzewski, S. Dapprich, A.D. Daniels, M.C. Strain, O. Farkas, D.K. Malick, A.D. Rabuck, K. Raghavachari, J.B. Foresman, J.V. Ortiz, Q. Cui, A.G. Baboul, S. Clifford, J. Cioslowski, B.B. Stefanov, G. Liu, A. Liashenko, P. Piskorz, I. Komaromi, R.L. Martin, D.J. Fox, T. Keith, M.A. Al-Laham, C.Y. Peng, A. Nanayakkara, M. Challacombe, P.M.W. Gill, B. Johnson, W. Chen, M.W. Wong, C. Gonzalez, J.A. Pople. *Gaussian 03, Revision B.03*, Gaussian Inc., Wallingford, CT (2004).
[40] M. Galle, R. Puchta, N.J.R. van Eikema Hommes, R. van Eldik. *Z. Phys. Chem.*, **220**, 511 (2006).
[41] R. Puchta, R. van Eldik. *Eur. J. Inorg. Chem.*, 1120 (2007).
[42] R. Puchta, R. Meier, R. van Eldik. *Aust. J. Chem.*, **60**, 889 (2007).
[43] R. Puchta, R. van Eldik. *J. Incl. Phenom. Macrocycl. Chem.*, **60**, 383 (2008).
[44] S. Begel, R. Puchta, R. van Eldik. *Beilstein J. Org. Chem.*, **9**, 1252 (2013).
[45] R.D. Shannon. *Acta Crystallogr. B*, **32**, 751 (1976).
[46] Nimag: 5.
[47] V. Seitz. Dissertation, Universität Erlangen-Nürnberg (2000).
[48] R. Puchta. Dissertation, Universität Erlangen-Nürnberg (2003).
[49] R. Puchta, M. Galle, N.J.R. van Eikema Hommes, E. Pasgreta, R. van Eldik. *Inorg. Chem.*, **43**, 8227 (2004).
[50] R. Puchta, N.J.R. van Eikema Hommes, R. van Eldik. *Helv. Chim. Acta*, **88**, 911 (2005).
[51] (a) M. Döring, E. Uhlig, K. Brodersen, A. Wolski. *Z. Anorg. Allg. Chem.*, **619**, 753 (1993); (b) M. Döring, H. Görls, E. Uhlig, K. Brodersen, L. Dahlenburg, A. Wolski. *Z. Anorg. Allg. Chem.*, **614**, 65 (1992); (c) M. Döring, E. Uhlig, L. Dahlenburg. *Z. Anorg. Allg. Chem.*, **578**, 58 (1989).
[52] R.W. Saalfrank, H. Maid, N. Mooren, F. Hampel. *Angew. Chem.*, **114**, 323 (2002); *Angew. Chem. Int. Ed.*, **41**, 304 (2002).
[53] I. Ravikumar, P.S. Lakshminarayanan, E. Suresh, P. Ghosh. *Beilstein J. Org. Chem.*, **5** (2009). doi:10.3762/bjoc.5.41.
[54] Y.K. Lau, P.P.S. Saluja, P. Kebarle, R.W. Alder. *J. Am. Chem. Soc.*, **100**, 7328 (1978).
[55] M. Klisch, P. Richter, R. Puchta, D.-P. Häder, W. Bauer. *Helv. Chim. Acta*, **90**, 488 (2007).
[56] R. Puchta, M. Galle, N.J.R. van Eikema Hommes. *Z. Naturforsch.*, **61b**, 1327 (2006).
[57] R. Puchta, A. Scheurer. *Z. Naturforsch.*, **65b**, 231 (2010).